

Investigation of Moving Angle of Power Take off Mechanism on the Efficiency of Wave Energy Converter

파력발전기의 동력인출장치의 회전각도가 효율에 미치는 영향 분석

H. T. Do¹, M. T. Nguyen¹, C. B. Phan¹, S. Y. Lee¹, H. G. Park² and K. K. Ahn^{2*}

도황팅 · 누옌밍치 · 판콩빙 · 이세영 · 박형규 · 안경관

Received: : 27 Jul. 2015, Revised: 25 Aug. 2015, Accepted: 27 Aug. 2015

Key Words : hydrostatic transmission(정유압 변속기); wave energy converter(파력 발전기); floating buoy(부표); power-take-off mechanism(동력인출장치).

Abstract: The hydraulic power-take-off mechanism (HPTO) is one of the most popular methods in wave energy converters (WECs). However, the conventional HPTO with only one direction motion has a number of drawbacks that limit its power capture capability. This paper proposes an adjustable moving angle wave energy converter (AMAWEC) and investigates the effect of the moving angle on the performance of the wave energy converter to find the optimal moving angle in order to increase the power capture capability as well as energy efficiency. A mathematical model of components from a floating buoy to a hydraulic motor was modeled. A small scale WEC test rig was fabricated to verify the power capture capability and efficiency of the proposed system through experiments.

Nomenclature

A_v : relief valve throttling area, m^2
 A_{CVO} : cross-section of the check valve CVO
 A_b : relief valve throttling area, m^2
 C_d : discharge coefficient
 C_D : drag coefficient in water
 D : bore diameter of cylinder, m
 D_{max} : maximum displacement of hydraulic motor, cc/rev
 f_i : random frequencies of wave component, Hz

g : gravitational acceleration, m/s^2
 m_b : mass of the floating buoy, kg
 m_s : mass of the moving shaft, kg
 n : adiabatic coefficient
 p_0 : pre-charged pressure, Pa
 p_2 : pressure high-pressure hose, Pa
 $S_A(f_i)$: spectral density of the represented sea states, m^2/s
 V_h : volume of the hoses, m^3
 V_0 : initial volume of the HPA, m^3
 $y(t)$: displacement of the floating buoy, m
 $Y(t)$: irregular wave displacement, m
 z : submerged level of the floating buoy, m
 α : moving angle of floating buoy
 α_M : displacement ratio of hydraulic motor
 α_o : optimal moving angle of floating buoy
 β : bulk modulus of oil, Pa
 ω : motor rotation speed, rpm
 Δf : increment of wave frequency, Hz
 Δp : pressure difference between the two ports of

* Corresponding author: kkahn@ulsan.ac.kr
 1 Graduate school of Mechanical and Automotive Engineering, University of Ulsan, Ulsan 44610, Korea.
 E-mail: dohoangthinh2010@gmail.com
 2 School of Mechanical Engineering, University of Ulsan, Ulsan 44610, Korea.

Copyright © 2015, KSFC

This is an Open-Access article distributed under the terms of the Creative Commons Attribution Non-Commercial License(<http://creativecommons.org/licenses/by-nc/3.0>) which permits unrestricted non-commercial use, distribution, and reproduction in any medium, provided the original work is properly cited.

the motor, Pa

η_{vM} : volumetric efficiency of hydraulic motor

η_{mM} : mechanical efficiency of hydraulic motor

ρ : density of water, kg/m³

$\varphi_{rand,i}$: random phases of wave component, Rad

v : wave velocity, m/s

1. Introduction

The demand for energy is rapidly increasing; fossil resources get scarcer and scarcer. Many studies in the field of wave energy and various technologies of wave energy conversion systems, or wave energy converters (WECs) are currently being developed, such as overtopping devices (for example, the Wave Dragon), attenuators (Pelamis) and point absorbers (WaveBob, OPT PowerBuoy), as noted in ¹⁾. The prior principle of WEC is that wave motion is used to create a high-pressure fluid, which is used to drive a hydraulic motor coaxially connected to an electric generator. One of the simplest and most popular wave energy converters is point absorber type, mentioned in ²⁾ and ³⁾. However, wave energy is absorbed in only one direction: either vertical or horizontal. Therefore, this limits the total efficiency of the converter. Heikkinen et al. in ⁴⁾ proposed a new structure of and cylindrical wave energy converters oscillating in two modes. This approach can absorb energy in two directions to improve the total efficiency, but similar to the seabed-mounted bottom-hinged wave energy converter in ⁵⁾, it still has some drawbacks, such as: difficulty in maintenance; corrosion and oil leakage.

To overcome the drawbacks of the above wave energy converters and enhance the total efficiency, an adjustable moving angle wave energy converter (AMAWEC) is proposed in this paper. Besides, the experiment was done in three conditions corresponding to weak, normal and strong wave conditions; and, moving angle is varied from 0 (vertical) to 20 degree to investigate an optimal moving angle of each wave condition.

The rest of this paper is organized as following:

section 2 describes the wave simulator and AMAWEC's test rig, section 3 presents the mathematical model of AMAWEC; section 4 shows the experiments and analysis of the experimental results. Finally, conclusions and future works are presented in section 5.

2. Description of wave simulator and adjustable moving angle wave energy converter

2.1 Wave simulator

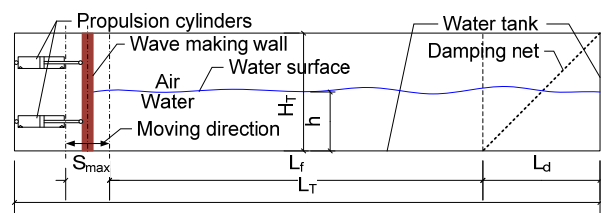


Fig. 1 Schematic diagram of wave simulator

A wave simulator with adjustable amplitude and frequency is employed, as in Fig. 1. The wave simulator includes a wave making wall moved by propulsion hydraulic cylinders, placed in a water tank. A slope damping net attached at the opposite side of the wave making wall can eliminate the reflex wave to avoid inexpectant noise. The motion of a wave making wall and cylinders are set up and controlled by a computer and sensors to achieve an exact wave amplitude and frequency.

Table 1 Parameters of wave simulator

Parameter		Symbol	Value
Water tank	Length	L_T	50m
	Width	W_T	20m
	Height	H_T	2m
Damping length		L_d	5m
Water depth		h	1m
Max. stroke of wave making wall		S_{max}	0.5m
Propulsion cylinder	Bore diameter	D_p	50mm
	Rod diameter	d_p	28mm
	Length	l_p	0.7m
	Quantity	q	10

The working principle of wave simulator in this research is rather similar to the wave maker in⁶⁾. The main parameters of the wave simulator are presented in Table 1.

Table 2 Parameters of AMAWEC

Parameter		Symbol	Value
Cylinder	Bore diameter	D	25mm
	Rod diameter	d	12mm
	Length	l	0.5m
Accumulator	Volume	V_0	3L
	Pre-charged press.	p_0	5bar
Hyd. motor	Displacement	D_m	12.5cc/rev

2.2 Adjustable moving angle wave energy converter

The test rig of AMAWEC includes two parts, as shown in Fig. 2: PTO part and hydraulic transmission part. In the PTO part, a floating buoy attached to a moving shaft can be moved by wave, as in the upper photograph of Fig. 2. The moving shaft is ensured to move in with low friction by rollers in a predefined moving angle α by an electric actuator.

The moving shaft connects to a hydraulic cylinder which functions as a hydraulic pump to generate pressurized fluid. The moving angle adjustment is carried out by a rotation mechanism with electric actuator and potential meter. The control signal is given by a PID closed-loop controller from a computer. The PTO part and hydraulic transmission part are supported by a frame and conjoined via hydraulic hoses. A low pressure hose lets low pressure fluid from tank to the hydraulic cylinder while a high pressure hose lets pressurized fluid from the cylinder go to high pressure accumulator and hydraulic motor of the hydraulic transmission part as in the lower photograph.

The hydraulic circuit of AMAWEC is shown in Fig. 3. When the cylinder is extended, fluid is sucked from the tank to the full bore chamber of the cylinder. The check valve CVI allows

low-pressure fluid from the low-pressure hose into the cylinder but prohibits the opposite direction. When the cylinder is compressed, fluid in the full bore chamber is pressurized and pumped to the high-pressure accumulator (HPA). The check valve CVO lets high-pressure fluid from the cylinder into the high-pressure hose to charge the HPA but prohibits the opposite direction. The hydraulic motor is driven by high-pressure fluid from the HPA. By employing HPA, the operation pressure is smoothed and the fluctuation of hydraulic motor velocity is reduced. The relief valve RLV₁ releases pressure in the HPA to protect the hydraulic circuit if the operating pressure becomes too high. A Magnetorheological (MR) brake is used to simulate the load of a generator. A torque and speed sensor is placed between the hydraulic motor and the “generator”– herein MR brake for output power calculation. Parameters of components of AMAWEC are shown in Table 2.

The data of wave, floating buoy motion, buoyant force, pressure of cylinder and accumulator, hydraulic motor’s flow rate, output torque and speed are collected from corresponding sensors to computer via a data acquisition card. A Matlab Simulink program is built for moving angle control and data processing.

3. Mathematical modeling of the adjustable moving angle wave energy converter

3.1 Wave Model

An irregular ocean wave can be represented as the sum of single waves as described by the Pierson–Moskowitz spectrum as in Fig. 4 from⁷⁾. Their irregular wave spectrum is represented by the significant wave height H_s and the peak wave period T_p .

An irregular wave can be generated as a sum of wave components as discussed in⁸⁾:

$$Y(t) = \sum_{i=1}^n \sqrt{2S_A(f_i)\Delta f} \sin(2\pi f_i t + \varphi_{rand,i}) \quad (1)$$

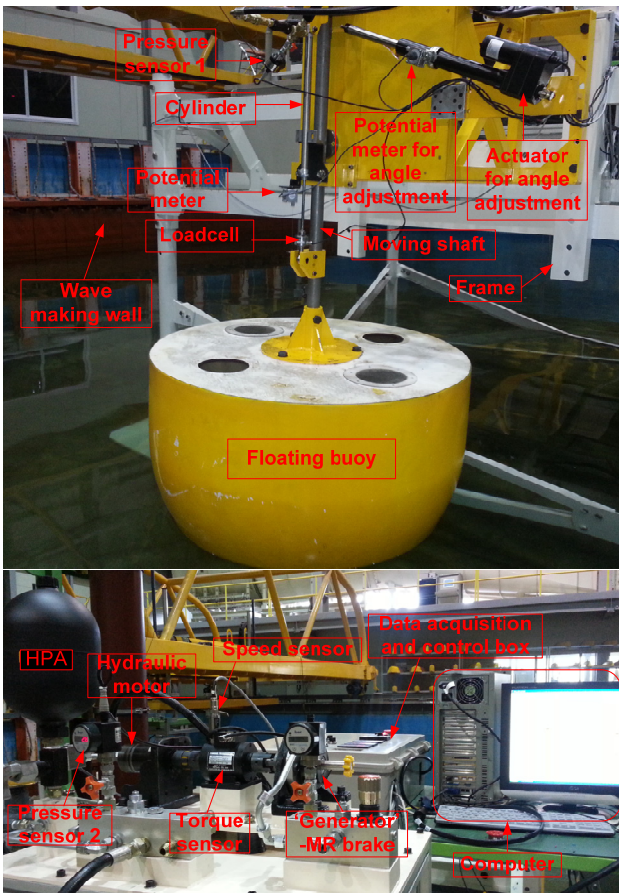


Fig. 2 AMAWEC test rig

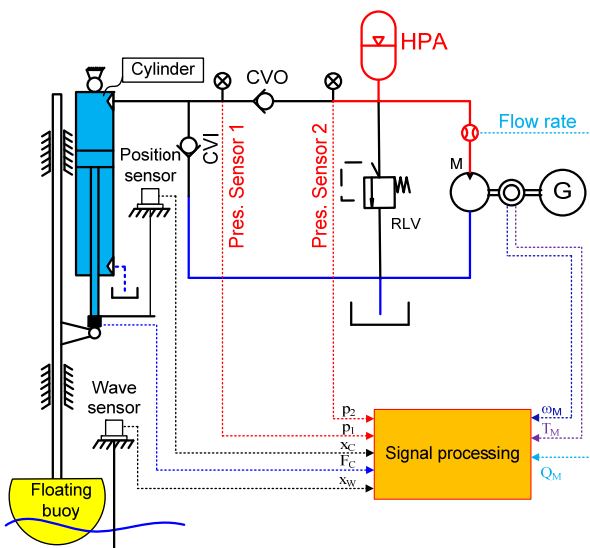


Fig. 3 Hydraulic circuit of AMAWEC

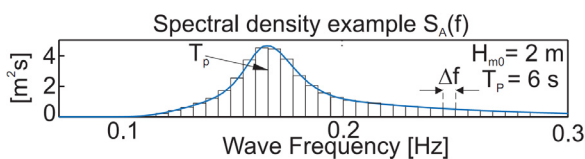


Fig. 4 Wave spectra for sea states

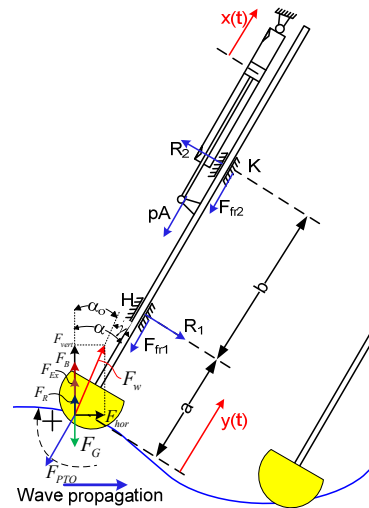


Fig. 5 Detail view and force analysis of PTOM

3.2 Hydrodynamic model of a floating buoy

The motion of a floating buoy can be described using the following equation:

$$(m_b + m_s) \ddot{y}(t) = F_w \cos \gamma - F_{PTO} \quad (2)$$

where F_{PTO} is the force to move the cylinder piston to make high-pressure fluid, and F_w is the resultant force from wave on the floating buoy, as in Fig. 5, included vertical component F_{vert} and horizontal component F_{hor} :

$$F_w = F_{vert} + F_{hor} \quad (3)$$

According to ⁹⁾, the vertical force exerted on the floating buoy can be represented as a superposition of three components: the hydrostatics force; the excitation force applied by an incoming regular wave to a fixed float; and the radiation force experienced by an oscillating float, which is the sum of the forces created by the motion of the other buoys floating on the water. Vertical force from the wave is defined as:

$$F_{vert} = F_B + F_{Ex} + F_R - F_G \quad (4)$$

Here, F_B is the buoyant force, F_{Ex} is the excitation force and F_R is the radiation force,

produced by an oscillating body creating waves on an otherwise calm sea.

The buoyant force F_B is calculated as:

$$F_B = \rho g V_s \quad (5)$$

Here, V_s is the volume of the floating buoy that is below the water surface, as in Fig. 6, defined as:

$$V_s = \begin{cases} \pi(3R-z)z^2/3, & 0 < z \leq R \\ 2\pi R^3/3 + \pi R^2(z-R), & R < z \leq R+h \end{cases} \quad (6)$$

The excitation force F_{EX} is expressed as in ¹⁰:

$$F_{EX} = 0.5\Gamma(\omega_w)H \sin \omega_w t \quad (7)$$

where $\Gamma(\omega_w)$ is the excitation force coefficient, which is dependent on the body's shape and the wave frequency (ω_w) as discussed in ^{8,9}, and H is the wave height (from peak to peak).

$$\Gamma(\omega_w) = \sqrt{2g^3 \rho B(\omega_w) / \omega_w^3} \quad (8)$$

The coefficient $B(\omega_w)$ depends on the wave frequency.

The radiation force is expressed as:

$$F_R = -(m_{Ad}\ddot{y} + b_{rad}\dot{y}) \quad (9)$$

where b_{rad} is the impulse response function describing the hydrodynamic damping. The term m_{Ad} represents the "added mass"; this term is included to account for the effect that, when a float oscillates, it appears to have a greater mass due to the water that is displaced along with it, as in ¹⁰.

F_G is the gravity force, calculated as:

$$F_G = (m_b + m_s)g \quad (10)$$

Horizontal force from a wave is called as drag force, defined as:

$$F_{hor} = 0.5\rho v^2 C_D A_{bh} \quad (11)$$

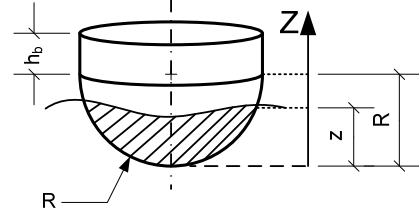


Fig. 6 Buoy shape and water level

where A_{bh} is the wet cross section of the buoy on a plane perpendicular to the direction of the wave:

$$A_{bh} = \begin{cases} R^2 [\arcsin((z-R)/R)] + 0.5 \sin 2[\arcsin((z-R)/R)] + 0.5\pi, & 0 < z \leq R \\ 0.5\pi R^2 + 2R(z-R), & R < z \leq R+h_b \end{cases} \quad (12)$$

3.3 Model of hydraulic cylinder

In this approach, a cylinder was employed as hydraulic pumps to convert the kinetic energy of a floating buoy into potential energy stored in the HPA. The floating buoys are moved by waves, and then fluid in cylinders is pressurized. Define $x(t)$ as the x -coordinate of the piston. The cylinder rod is fixed to the floating buoy, so:

$$\dot{x}(t) = \dot{y}(t) \quad (13)$$

As the piston of the cylinder moving, the continuity equation of the bore chamber is:

$$dp_1 / dt = \beta (A_p \dot{x} + Q_{CVI} - Q_{CVO}) / (A_p L_0 - A_p x_i) \quad (14)$$

where $A_p L_0$ is initial volume of the bore chamber; A_p is the piston area in m^2 :

$$A_p = \pi D^2 / 4 \quad (15)$$

Q_{CVI} is the input flow rate from the tank to the cylinder via check valve CVI :

$$Q_{CVI} = \begin{cases} C_d A_{CVI} \sqrt{2|p_t - p_1| / \rho}, & \text{if } p_t > p_1 \\ 0, & \text{else} \end{cases} \quad (16)$$

Q_{CVO} is the output flow rate from the cylinder to the HPA via check valve CVO :

$$Q_{CVO} = \begin{cases} C_d A_{CVO} \sqrt{2|p_1 - p_2| / \rho}, & \text{if } p_1 > p_2 \\ 0, & \text{else} \end{cases} \quad (17)$$

p_1 is the pressure at the cylinder port defined by Eq. (14); p_2 is the pressure of the fluid in the high-pressure hose;

The cylinder force is calculated as:

$$F_{PTOi} = \Delta p_{1t} A_p + F_{fric} \quad (18)$$

Where

$$\Delta p_{1t} = p_1 - p_t \quad (19)$$

F_{fri} is the friction force of the cylinder, defined as:

$$F_{fric} = |\Delta p_{1t} A_p| (1 - \eta_c) \quad (20)$$

The cylinder friction F_{fric} is defined such that the cylinder has a friction coefficient η_c .

3.4 Modeling and calculation of the HPA

In the proposed system, we employed a bladder accumulator, which was filled with nitrogen gas. According to ¹¹⁾, the nitrogen gas is assumed to compress and expand based on the adiabatic gas law:

$$pV^n = p_0 V_0^n = p_{\max} V_{\min}^n \quad (21)$$

Then the fluid volume in the HPA is derived as:

$$V_{HPA} = \begin{cases} 0, & \text{if } p_2 \leq p_0 \\ V_0 (1 - p_0 / p_2)^{1/n}, & \text{else} \end{cases} \quad (22)$$

3.5 Model of connecting hose

Using the flow continuity equation, the pressure in the high-pressure hose is expressed as:

$$dp_2 / dt = \beta (Q_{CVO} - Q_{HPA} - Q_r - Q_m) / V_h \quad (23)$$

where Q_{CVO} represents the flow rate through the check valves CVO , as formulated in Eq. (17); Q_{HPA} is the flow rate into the HPA, derived based on Eq. (22) as:

$$Q_{HPA} = \dot{V}_{HPA} = \begin{cases} 0, & \text{if } p_h \leq p_0 \\ V_0 (1 - p_0 / p_h)^{(1-n)/n} p_0 \dot{p}_h / (n p_h^2), & \text{else} \end{cases} \quad (24)$$

Q_r is the flow rate through the relief valve RLV. According to ¹²⁾, Q_r can be expressed as:

$$Q_r = \begin{cases} 0, & \text{if } \Delta p_{2t} \leq \Delta p_{set} \\ C_d A_v \sqrt{2 \Delta p_{2t} / \rho}, & \text{if } \Delta p_{2t} \geq \Delta p_{set} \end{cases} \quad (25)$$

Q_m is the actual flow rate of the hydraulic motor as in Eq. (28), and Δp_{2t} is the pressure difference between the high-pressure hose and low-pressure hose, which is considered to be the pressure in the tank p_t :

$$\Delta p_{2t} = p_2 - p_t \quad (26)$$

3.6 Model of the hydraulic motor

The ideal flow rate of the hydraulic motor is defined as:

$$Q_{mi} = \alpha_M D_{\max} \omega_M \quad (27)$$

The actual flow rate and actual output torque of the piston hydraulic motor are expressed by Eq. (28), (29), respectively.

$$Q_m = Q_{mi} / \eta_{vM} \quad (28)$$

$$T_m = \alpha_M \Delta p D_{\max} \eta_{tM} \quad (29)$$

Here, Q_l and T_l are the loss flow rate and the loss torque of the pump, respectively, which were discussed in ¹³⁾.

4. Experiment

4.1 Wave condition and energy flux

Experiments are carried out as following: for each wave condition, the moving angle α of floating buoy is adjusted from 0 to 20°, with the step of 2°. The experiment duration each angle is 30s. There are three wave conditions: No. 1, No. 2 and No. 3 corresponding to weak, medium and strong are set up. According to ref.¹⁴, energy flux in 1 period for shallow-water of the water tank is expressed as:

$$E = \rho g^{3/2} H^2 \sqrt{hTb} / 8 \tag{30}$$

Based on the parameters in Table 3, the result of energy flux in 1 period and 30s are calculated as in Table 4.

Table 3 Parameters of floating buoy and water

Water density ρ [Kg/m ³]	Gravity g [m/s ²]	Buoy width b [m]	Water depth h [m]
1000	9.81	0.9	1

4.2 Investigation of the optimal moving angle

The experimental results of typical experiments as well as some important results of all experiments are presented. In each condition, the moving angle α of floating buoy is changed from zero to 20°. By changing the moving angle, the best efficiency regarding to the optimal moving angle α_o is found out. For each wave condition, the optimal moving angle α_o would be different.

Table 4 Wave energy flux

Wave condition	Wave height H[m]	Wave period T[s]	Wave length λ [m]	Energy in 1 period [J]	Energy in 30s [J]
No. 1	0.124	2.4	7.468	127.559	1594.49
No. 2	0.151	2.8	8.991	220.682	2364.47
No. 3	0.205	1.8	5.145	261.478	4357.98

Firstly, detailed experimental results of *conventional moving angle* (0°) and *optimal moving angle* in wave condition No. 3 are considered as

typical experimental results. In here, based on experimental results, the optimal moving angle in wave condition No. 3 is 12°. The comparison of detailed experimental results of conventional moving angle (0°) and optimal moving angle (12°) in wave condition No. 3 are presented in through Fig. 7-Fig. 14.

Fig. 7 and Fig. 8 show wave and buoyant displacement, and buoyant speed in both cases of conventional moving angle (0°) and optimal moving angle (12°). With the same wave condition, buoyant displacement is better or longer in optimal moving angle case.

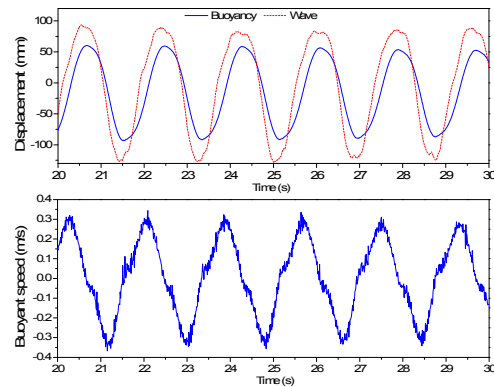


Fig. 7 Wave and buoyant displacement, and buoyant speed in conventional moving angle (0°)

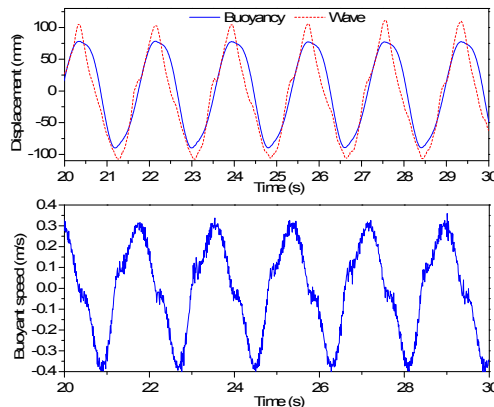


Fig. 8 Wave and buoyant displacement, and buoyant speed in optimal moving angle (12°)

Comparison of flow rate of hydraulic motor and buoyant force in optimal moving angle are a higher than in conventional moving angle, as shown in Fig. 9.

The performance of AMAWEC is displaced by driven torque and driven speed of the hydraulic motor, compared in Fig. 10. Driven torque looks not so different, however driven speed in optimal moving angle is a higher than in conventional moving angle.

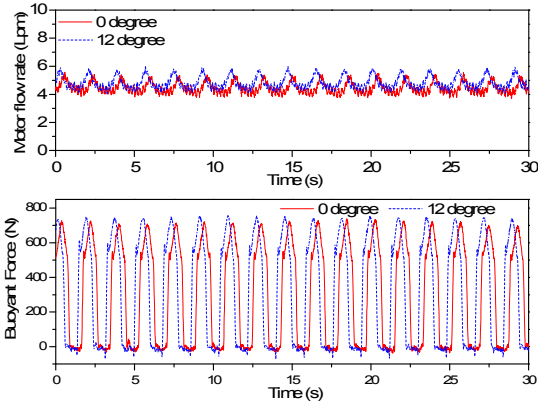


Fig. 9 Comparison of flow rate and buoyant force in conventional moving angle (0^0) and optimal moving angle (12^0)

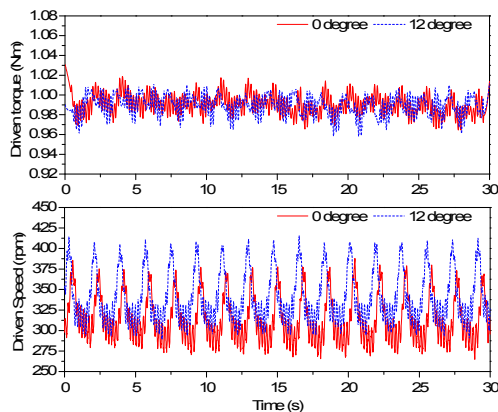


Fig. 10 Comparison of output torque and speed in conventional moving angle (0^0) and optimal moving angle (12^0)

Input power is calculated by the product of buoyant force and buoyant speed, while output power is calculated by the product of driven torque and driven speed. Then, the integral of input/output power is defined as input/output energy. Input/output power and input/output energy in both conventional moving angle (0^0) and in optimal moving angle (12^0) are shown in Fig. 11 and Fig. 12. In both cases, the input power varies in

wide range, but thanks to effect of the HPA, the output power is steady.

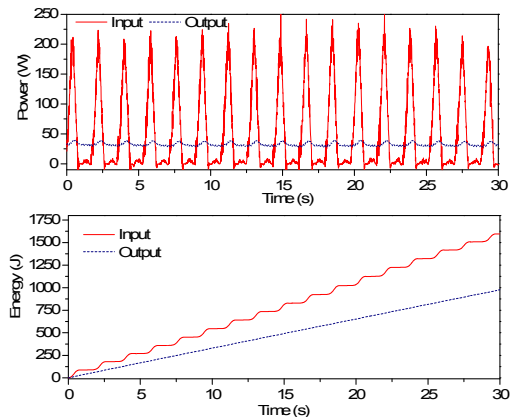


Fig. 11 Input/output power and input/output energy in conventional moving angle (0^0)

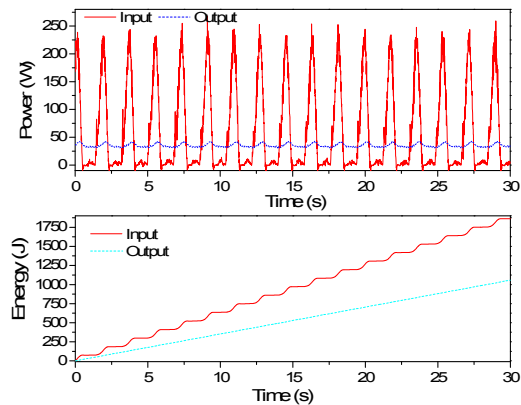


Fig. 12 Input/output power and input/output energy in optimal moving angle (12^0)

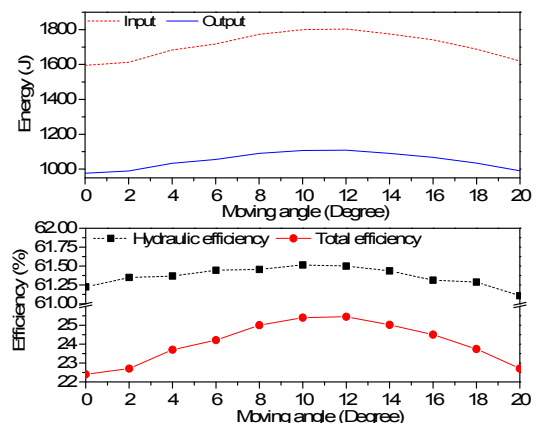
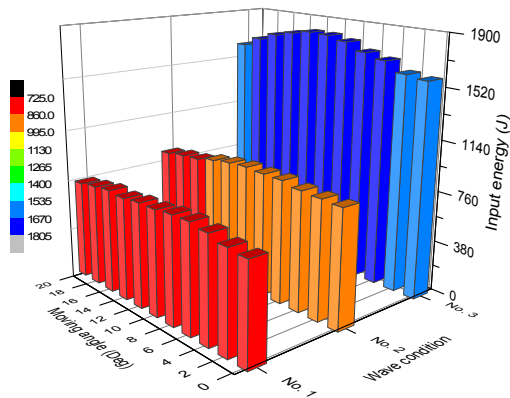


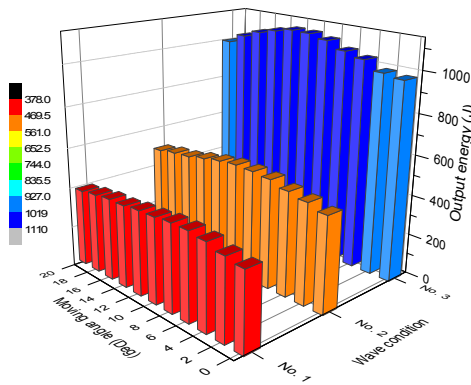
Fig. 13 Comparison of input/output energy and efficiency regarding to moving angle

Input/output energy and efficiency regarding to moving angle α (from zero to 20 degree) are shown

in Fig. 13. The tops of input and output energy are at 12 degree, called as optimal moving angle. It means that the wave energy converter can perform best at the optimal moving angle: more energy absorbed (from wave) and more output energy generated (by generator); therefore, the total efficiency can be improved. The output energy in 30s of conventional moving angle case is 976J, whereas it is 1109J in the case of optimal moving angle. So that 13.6% of output energy can be improved. The hydraulic efficiency of AMAWEC is calculated as the ratio of output energy and input energy. As in Fig. 13, the hydraulic efficiency is almost constant. The total efficiency of AMAWEC is calculated as the ratio of output energy and wave energy flux, calculated in Table 4. Fig. 13 indicates that the total efficiency regarding to moving angle achieves the top value (25.45%) at optimal moving angle compared to 22.40% at conventional moving angle (0^0).



(a) Input energy

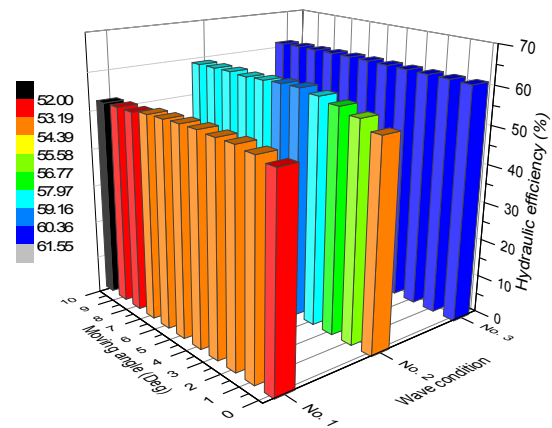


(b) Output energy

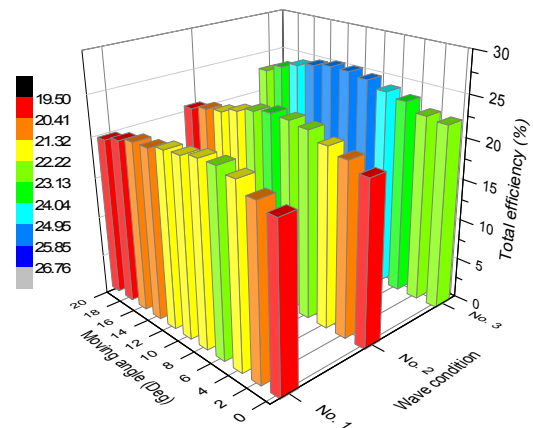
Fig. 14 Input/output energy regarding to moving angle and wave conditions

Experiments of other wave conditions are also carried out. Fig. 14 presents the input/output energy regarding to moving angle and wave conditions. The top of input/output energy occurred at the optimal moving angle. It can be found that the optimal moving angle of each wave condition is different from the others. In here, the optimal moving angle of wave conditions No. 1, No. 2 and No. 3 is 6^0 , 10^0 and 12^0 , respectively.

The efficiencies of AMAWEC regarding to moving angle and wave conditions are shown in Fig. 15. The hydraulic efficiency is almost constant regarding to moving angle but it is better with the stronger wave conditions. Nevertheless, the total achieves top value regarding to moving angle as well as better value with the stronger wave conditions.



(a) Hydraulic efficiency



(b) Total efficiency

Fig. 15 Efficiencies of AMAWEC regarding to moving angle and wave conditions

After all, this is an encouraging result that efficiency of wave energy converter can be improved by finding optimal moving angle of floating buoy.

5. Conclusions and future works

This research proposed an AMAWEC, in which, the moving angle can be adjusted to investigate the optimal moving angle according to wave conditions. All components of AMAWEC were mathematically modelled. Moreover, experiments of three wave conditions and the adjustment of moving angle from zero to 20° were carried out. The experimental results illustrated that there exists an optimal moving angle which made the AMAWEC shown best performance. Typically, the experimental result in wave condition No. 3 indicated that the output energy can be improved 13.6% by operating at optimal moving angle, and the total efficiency at this angle is 25.45% compared to 22.40% at conventional moving angle (0°).

The experimental results of the AMAWEC were encouraging to develop the WEC in this way with the demand of more efficiency. Hence, the future works as the next step of this project, the following issue would be considered. First, methods to automatically achieve optimal moving angle need to be proposed. Second, a full scale of with multi-point absorber WEC needs to be developed. This work has been done as the 2nd year stage of this project. And third, pressure coupling principle would be applied for speed control and improving the transmission efficiency. Because of this, a variable displacement hydraulic motor would be employed instead of the fixed displacement one. Finally, new concept of AMAWEC has been currently investigated and developed.

Acknowledgment

This work was partly supported by the New & Renewable Energy of the Korea Institute of Energy

Technology Evaluation and Planning (KETEP) grant funded by the Korea government Ministry of Trade, Industry and Energy (G031518511) and by the project titled 'R&D center for underwater construction robotics', funded by the Ministry of Oceans and Fisheries (MOF) and Korea Institute of Marine Science & Technology Promotion (KIMST), Korea (PJT200539).

References

- 1) G. Nielse, M. Andersen, K. Argyriadis, S. Butterfield, N. Fonseca, T. Kuroiwa, M. L. Boulluec, S. J. Liao, S. R. Turnock, J. Waegter, "Specialist Committee V.4: Ocean Wind and Wave Energy Utilization", 16th Int. Ship and Offshore Structures Congress, pp. 165-211, 2006.
- 2) J. A. Oskamp, H. T. Özkan-Haller, "Power calculations for a passively tuned point absorber wave energy converter on the Oregon coast," *Renewable Energy*, Vol.45, pp. 72-77, 2012.
- 3) A. S. Zurkinden, F. Ferri, S. Beatty, J. P. Kofoed, M. M. Kramer, "Non-linear numerical modeling and experimental testing of a point absorber wave energy converter," *Ocean Engineering*, Vol.78, pp.11-21, 2014.
- 4) H. Heikkinen, M. J. Lampinen, J. Böling, "Analytical study of the interaction between waves and cylindrical wave energy converters oscillating in two modes," *Renewable Energy*, Vol.50, pp. 150-160, 2013.
- 5) M. Folley, T. W. T. Whittaker and J. van't Hoff, "The design of small seabed-mounted bottom-hinged wave energy converter," *Proc. of 7th European Wave and Tidal Energy Conference*, Portugal, 2007.
- 6) M. Anbarsooz, M. Passandideh-Fard, M. Moghiman, "Fully nonlinear viscous wave generation in numerical wave tanks," *Ocean Engineering* Vol.59, pp. 73-85, 2013.
- 7) R. H. Hansen, T. O. Andersen and H. C. Pedersen "Model based design of efficient power take-off systems for wave energy converters," 12th Scandinavian International

- Conf. on Fluid Power, Finland, 2011.
- 8) M. J. Ketabdari and A. Ranginkaman "Simulation of Random Irregular Sea Waves for Numerical and Physical Models Using Digital Filters," *Transaction B: Mechanical Engineering*, Vol.16 No.3, pp. 240-247, 2009.
 - 9) J. Falnes, *Ocean Waves and Oscillating Systems*, Cambridge University Press, Cambridge, 2002.
 - 10) C. Cargo, A. Plummer, A. Hillis and M. Schlotter "Optimal design of a realistic hydraulic power take-off in irregular waves," *Centre of Power Transmission and Motion Control- University of Bath*, 2011.
 - 11) M. G. Rabie, *Fluid Power Engineering*, McGraw-Hill, 2009.
 - 12) M. J. Pinches and J. G. Ashby, *Power Hydraulics*, Englewood Cliffs, NJ: Prentice-Hall, 1988.
 - 13) T. H. Ho and K. K. Ahn, "Modeling and simulation of a hydrostatic transmission system with energy recuperation using a hydraulic accumulator," *JMST*, Vol.24, No.5, pp. 1163-1175, 2010.
 - 14) M. E. McCormick, *Ocean Engineering Mechanics with Applications*, Cambridge University Press, 2010.